Electrostatic control of the proximity effect in the bulk of semiconductor-superconductor hybrids

van Loo, Nick; Mazur, Grzegorz P.; Dvir, Tom; Wang, Guanzhong; Dekker, Robin C.; Lemang, Mathilde; Sfiligoj, Cristina; Bordin, Alberto; van Driel, David; Kouwenhoven, Leo P.

DOI
10.1038/s41467-023-39044-w

Publication date
2023

Document Version
Final published version

Published in
Nature Communications

ADVANCED OPTICAL MATERIALS
www.advopticalmat.de

Large Polaron Conduction, Photoconductivity, and Photochromism in GdO_xH_{3-2x} Oxyhydride Thin Films

Giorgio Colombi, Bart Boshuizen, Diana Chaykina, Leyi Hsu, Herman Schreuders, Tom J. Savenije, and Bernard Dam**

At ambient conditions, rare-earth oxyhydride thin films show reversible photochromism and photoconductivity, while their mechanism and relation are still unclear. In this work, this question is explored with in situ time-resolved measurements of both optical and transport properties of Gd-based oxyhydride thin films. It is found that p-type large polaron conduction is the initial mechanism of charge transport; however, upon photo-darkening, a 10^4-fold increase of conductivity occurs, and n-type carriers become dominant. Further, photochromism and photoconductivity are shown to originate from a single process, as indicated by the fact that the photoconductivity is exponentially proportional to the increase of optical absorption. This exponential relation, notably, cannot stem from any of the optically absorbing species thought responsible for photochromism and, therefore, suggests that their formation is accompanied by a concerted increase of negative charge carriers in the Gd oxyhydride films.

1. Introduction

Within the mixed-anion material class,[1] rare-earth (RE) oxyhydride thin films stand out because of their reversible photochromism and photoconductivity at ambient conditions, making them promising candidates as inorganic smart coating for windows and sensors.[2–4] Photochromism and photo-conductivity in polycrystalline rare-earth oxyhydride thin films were first reported in 2011 on Y-based compounds.[5] Since then, several other REs (RE=Sc, Y, Nd, Sm, Gd, Dy, Er)[6–10] were found to form photochromic oxyhydride thin films, suggesting that these properties are rather general to the whole material class. Common to all of them is the REO_xH_{3-2x} composition and a crystal structure based on the CaF_2-type lattice.[7] Here, the oxide O^{2-} and hydride H^- anions preferentially occupy the more stable tetrahedral interstitial sites, and after those are filled, the remaining H^- fraction occupies the octahedral interstitials.[11,12]

The composition of the oxyhydride and the deposition conditions were found to influence the extent and the speed of photochromism,[13–15] however, the general presence of the phenomenon indicates that its origin is intrinsic to the RE oxyhydride thin film material. While there is no definitive agreement on the photochromic mechanism, most research converges toward the idea that structural rearrangements enabled by the H^- (local) mobility[16] and/or reactivity are at the heart of photochromism. In this sense, it was proposed that photodarkening depends on the segregation of an optically absorbing phase,[17,18] and a reversible change in the H-sub-lattice upon illumination was indirectly observed via muon spin rotation spectroscopy (μSR).[19] Additionally, while the photo-darkening could be induced even at a temperature of 4K,[20] temperature-dependent measurements on aliovalent Ca-substituted Y oxyhydrides showed that the bleaching is a thermally activated process with fixed activation energy and attempt frequency proportional to the number of anion-vacancies.[21] Notably, epitaxially grown films darken upon illumination, but the reverse bleaching process appears kinetically impaired.[22]

Despite the interest in this class of materials, in their photochromic properties, and later in their H^- ionic conduction, very little research has been spent toward the study of their photoconductivity. In fact, at the time of writing, no other study managed to reproduce the results originally presented by Mongstad et al.[5] on Y oxyhydride films, namely a 10-fold reduction of the resistance upon illumination, followed by partial reversibility in the dark. Nonetheless, reliable information on the conductivity

G. Colombi, B. Boshuizen, D. Chaykina, L. Hsu, H. Schreuders, B. Dam
Materials for Energy Conversion and Storage
Department of Chemical Engineering
Delft University of Technology
Van der Maasweg 9, Delft NL-2629HZ, The Netherlands
E-mail: g.colombi@tudelft.nl; b.dam@tudelft.nl

D. Chaykina
Fundamental Aspects of Materials and Energy
Department of Radiation Science and Technology
Faculty of Applied Sciences
Delft University of Technology
Mekelweg 15, Delft NL-2629 JB, The Netherlands

T. J. Savenije
Opto-electronic Materials
Department of Chemical Engineering
Delft University of Technology
Van der Maasweg 9, Delft NL-2629HZ, The Netherlands

The ORCID identification number(s) for the author(s) of this article can be found under https://doi.org/10.1002/adom.202202660

DOI: 10.1002/adom.202202660

and photo-conductivity of these thin films is (i) essential to evaluate their employability as solid-state ionic conductors in any electrochemical devices, (ii) a necessary prerequisite for any further tuning of their ionic/electronic transport properties, and (iii) a potential source of insight on the photochromic mechanism. From a more fundamental perspective, understanding the electrical transport in the RE oxyhydrides might help to further assess to which extent their properties resemble the related REH_x hydride systems, which have been extensively investigated in view of the metal-to-insulator transition that occurs upon a change of H-content.[23–26]

In this work, we present time-dependent measurements of optical and transport properties, including Hall-effect (HE). While in this work we focus on Gd-based oxyhydride thin films, the comparable photoconductivity of Y-based oxyhydrides,[5,15,22] and the general occurrence of photochromism, suggest that the conclusions drawn here might hold in general for the entire family of photochromic RE oxyhydride thin films. When the films are in their transparent (as-sputtered) state, we identify the mechanism of charge transport as p-type large-polaron conduction. Upon photodarkening, however, the conductivity increases by several orders of magnitude, this time dominated by negative charge carriers. Further, photochromism and photoconductivity appear connected by an exponential relation, which indicates a single origin, and yet cannot be explained by the sole segregation of a conductive optically absorbing phase.

2. Experimental Section

2.1. Sample Preparation

Gd-based REH_2 thin films (thickness $d \approx 300$ nm) were prepared by reactive magnetron sputtering of a 2-inch Gd target (MaTeck Germany, 99.9% purity) in a Ar/H_2 (6N purity) atmosphere. The deposition chamber was kept at a base pressure below 1×10^{-6} Pa. During deposition the total gas flow was fixed at 40 sccm with an Ar/H_2 gas ratio of 7:1, while the total deposition pressure (p_{dep}) was set to 0.75 Pa by means of a control gate valve mounted at the inlet of the pumping stage. Plasma excitation was sustained by 175W DC power supply. All samples were grown at room temperature on UV-grade fused silica (f-SiO_2) in a single deposition to guarantee a high homogeneity among them. The as-deposited REH_2 thin films were then oxidized in ambient conditions by exposure to air. Because the air-oxidation is largely a self-limiting process,[13,27] the samples were given a 14 + day rest period before further characterization.

2.2. Contact Deposition

To guarantee Ohmic metal-semiconductor junctions during transport measurements, the deposition of additional contact layers was needed. The following multilayer (in order, from the sample surface) was found to be optimal: 100 nm YH_2, 100 nm Cr, 100 nm Au.

Notably, during pilot experiments with sub-optimal contacts, it was observed that the UV exposure promoted the degradation of the contact-oxyhydride interface when different metals were used for the first layer (e.g., Y, Gd, GdH_2), leading to incomplete reversibility of both photochromism and photoconductivity. We suspect H-loss from the film to the contact to be the driver of this degradation. To further minimize the contact-oxyhydride interaction and the systematic errors during transport measurements,[28] the contacts were deposited at the corners of a 7×7 mm square, and their size was kept to a minimum of around 0.5 mm^2 (see Supporting Information, Section II for additional details).

2.3. Sample Characterization

Figure 1 shows a schematic of the experimental setup used to simultaneously measure optical transmittance and transport properties under the same temperature, vacuum, and illumination conditions. To achieve that, two samples were placed in connected vacuum chambers (pressure $\backsim 10^{-1}$ mbar) and kept at the same temperature by independent backplate heaters with a PID control loop. Specific setups were then used to measure their optical and electrical properties.

The optical transmittance, $T(\lambda)$, and reflectance, $R(\lambda)$, were measured at normal incidence with a custom built fiber-based spectrometer equipped with a white source (DH-2000BAL, Ocean Optics) and two Si-based energy dispersive spectrometers (HR4000 and Flame, Ocean Optics). The wavelength range was approximately 250–1000 nm, and the time resolution 30s. Combining transmittance and reflectance, the absorption coefficient was calculated according to: $\alpha(\lambda) = -ln[T(\lambda)/(1 - R(\lambda))]/d$.[29] Reflectance measurements were not possible when the temperature cell was installed in the instrument.

Resistance and HE were measured in a square Van der Pauw[28] geometry using an H50 HE current(voltage) source(meter), a commercial system from *MMR Technologies* that operates in a nominal resistance range of $10^2 - 10^{10}$ Ω, and with a time resolution of approximately 3min. A permanent magnet of 850G was used in the HE measurements.

Photochromism and photo-conductivity were triggered by two narrow-band LED calibrated to deliver the same intensity at the sample surface ($\lambda = 385$ nm, $I = 75$ mWcm^{-2}). Note that while light intensity does not need to be homogeneous for transmittance, which was probed in a central spot of $\backsim 2mm^2$, that is not the case for the transport measurements, which probe the entire sample area. To guarantee a homogeneous light intensity over the whole sample surface, a set of optical elements was installed in front of both LEDs following the principle of Köhler illumination.

Knowing that regions of RE oxyhydrides films that were previously exposed to light suffer from a so-called "memory effect",[5] namely a slower bleaching speed compared to a non-illuminated area, all the measurements presented here correspond to the first cycle of photo-darkening and bleaching of otherwise virgin (i.e., as-deposited) samples. Throughout this work, all values of averaged transmittance, reflectance, and absorbance refer to the interval λ: [450, 1000] nm.

3. Results and Discussion

3.1. Large-Polaron Conduction in Gd Oxyhydrides

In this section, we show that electronic transport in RE oxyhydride thin films occur as large-polaron conduction, as indicated

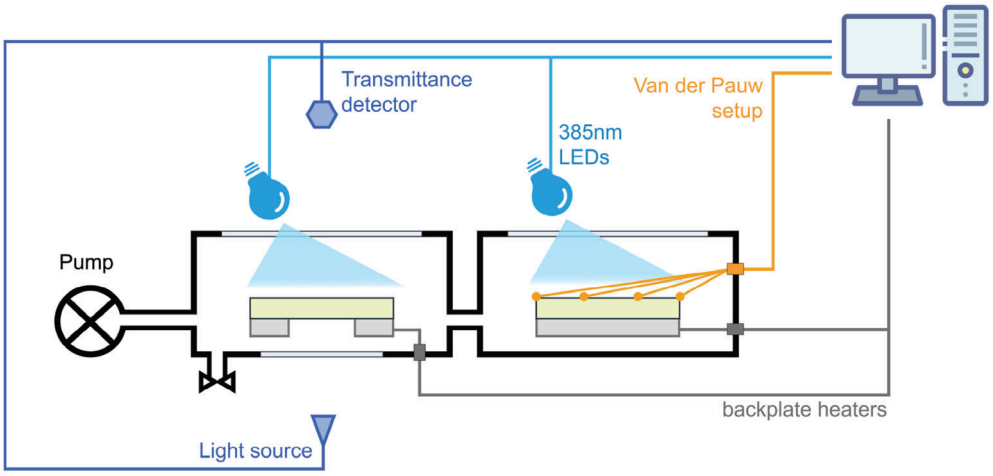

Figure 1. Schematics of the experimental setup used in this work. Optical transmittance and transport properties can be measured simultaneously under the same illumination, temperature, and vacuum conditions.

by HE results. Before delving in the results, we briefly discuss the context of these measurements.

In general, one distinguishes between coherent and incoherent electronic transport. Coherent transport envisions the carrier motion to be free, only occasionally disrupted by scattering events. Consequently, the carrier mobility decreases with increasing temperature, with typical values greatly exceeding 1 $cm^2\ s^{-1}\ V^{-1}$. Coherent transport is characteristic of free carrier conduction, and is also observed in the case of large polarons due to their large effective mass.[30] In contrast, incoherent transport—typical of small-polarons—envisions the carriers making occasional jumps between localized regions in the material. In this case, the mobility depends on the activation energy needed for the jump and thus rises with increasing temperature; typical values are well below 1 $cm^2\ s^{-1}\ V^{-1}$.[31]

HE measurements are an insightful tool to investigate the transport properties of a semiconductor, and are routinely employed to identify the dominant carrier polarity (i.e., electrons $\square_e$, or holes $\square_h$), and to quantify their density ($n_{e/h}$) and drift mobility ($\mu_{e/h}$).[32] However, this is only true in the special case of free carriers, meaning coherent transport within a band that is much wider than $k_B T$. In this common limit, the Hall mobility (μ_H) well approximates the actual drift mobility of the charge carriers and one can extract accurate information from the HE without additional knowledge on the material local/electronic structure. This is not the case for small(large) polaron conduction, which implies energy localization in states(narrow bands), as well as an influence of the local electrostatic potential on the direction of the polaron motion. The latter effect is particularly important in structures of low symmetry and can even lead to anomalous signs in the HE voltage. In this work, due to the fcc crystal symmetry of the RE oxyhydrides, we expect the sign of the Hall voltage to be consistent with the polarity of the charge carriers in case of polaron conduction. Similarly, the influence of temperature on the Hall mobility is expected to reflect the type of polarons, large ($d\mu_H/dT < 0$) or small ($d\mu_H/dT > 0$), even though Hall and drift mobilities might differ from one another in magnitude and exact temperature dependence.[31]

With this background in mind, the Gd oxyhydride Hall mobility and Hall carrier density are extracted considering a perfectly homogeneous film, and free carriers of a single polarity (see Supporting Information, Section I for additional information). In all our measurements, we find the Hall voltage (V_H) to have a positive sign, indicating that holes are the dominant charge carrier in these Gd oxyhydride thin films. The corresponding Hall mobility and Hall carrier density are shown in **Figure 2**. Considering the large optical bandgap, the found carrier density ($n_h \approx 10^{11} - 10^{12}\ cm^{-3}$) indicates a significant level of doping. This is in line with an high concentration of point defects expected in view of the high porosity of the films, and from the out-of-equilibrium fast oxidation in air. Because of that, we also expect a significant presence of ionized impurities and large line/volume defects; thus, the measured Hall mobility ($\mu_h \approx 10^3 - 10^4\ cm^2\ V^{-1}\ s^{-1}$) appears surprisingly high.[33–37] It is important to note here that even if the assumption of a single carrier were not verified, that would lead to an under-estimation of the carrier mobility (Figure S4, Supporting Information). Similarly, an overestimated material resistivity (for example due to contact resistance) would lead to an under-estimation of the carrier mobility. Therefore, the high Hall mobility of the Gd oxyhydrides cannot be traced back to any obvious experimental artifact. It must follow that the assumption of free carriers was faulty, indicating by exclusion a polaronic conduction mechanism.

The temperature dependence of conductivity, Hall carrier density, and Hall mobility gives further inside on the mechanism of charge transport in these Gd oxyhydride thin films. As the temperature increases, the total conductivity increases due to a net increase in carrier density. Conversely, the carrier mobility decreases. We rule out any significant ionic contribution to the values presented here, as the ionic H^- conductivity reported in LaO_xH_{3-2x} powders is (i) orders of magnitude smaller ($\sigma_{H^-} < 10^{-6}\ Scm^{-1}$), and (ii) a temperature activated process, thus, at odds with the decrease of mobility measured for increasing temperature.[16]

The limited temperature interval, due to sample instability above $\backsim 350\ K$ (see Supporting Information, Section III), makes

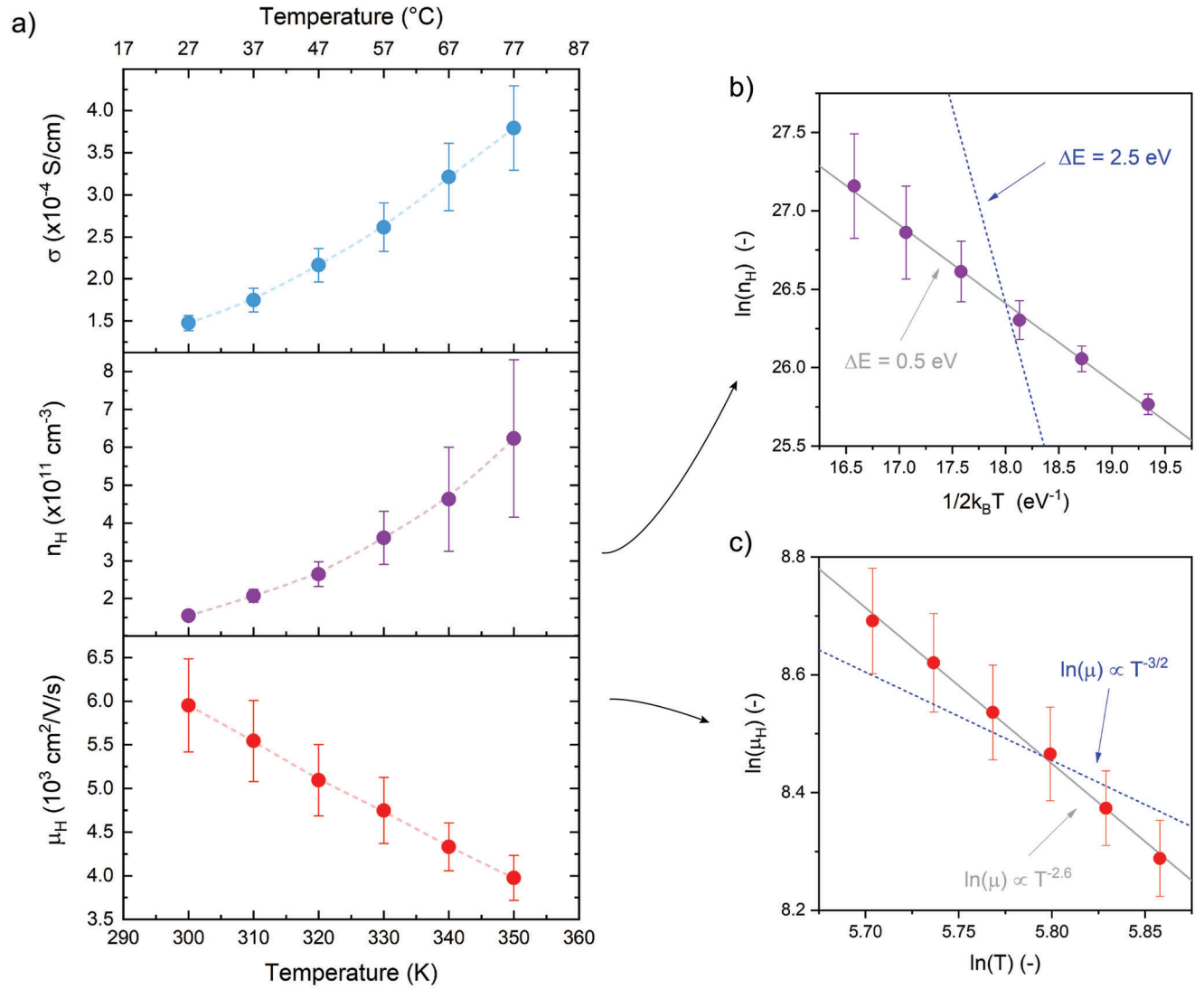

Figure 2. a) Temperature dependence of conductivity, carrier density, and Hall mobility of reactively sputtered Gd oxyhydride thin films. Dashed lines are a guide for the eyes. b) Fit of $n_H(T)$ based on the ideal relation that follows from a Fermi-Dirac distribution of the occupied/unoccupied states. The slope, ΔE, indicates the energy distance between the main in-gap electron acceptor level and the valence band (see text). For comparison, the blue dashed line gives the trend expected for an intrinsic semiconductor, where the slope reflects the electronic bandgap (~2.5 eV). c) Fit of $\mu_H(T)$ based on an exponential relation with the temperature. For comparison, the blue dashed line gives the trend expected in case of ideal free-carriers conduction.

it difficult to quantitatively discuss any material-specific temperature dependence; however, a fit of $n_H(T)$ based on the ideal relation that follows from a Fermi–Dirac distribution of the occupied/unoccupied states, $n \propto \exp(-\Delta E/2k_BT)$,[33] indicates that the material is not an intrinsic semiconductor. We find $\Delta E \sim 0.5$ eV (Figure 2b), which is clearly smaller than the optical gap and indicates the presence of deep states that, in view of the positive Hall potential, must act mainly as electron acceptors (i.e., hole donors). The chemical nature of these defects remains unclear, but we note that in the related REH_x hydride compounds the spare electron of H^- is known to shift to a vacant octahedral interstitial site and something similar might be happening in the RE oxyhydrides.[25]

Finally, the decrease of mobility with increasing temperature is typical of coherent electron transport and can be rationalized in terms of increasing phonon-scattering. We note that μ_H is negatively affected by the temperature (Figure 2c) to a greater extent compared to the ideal free carriers case, $\ln(\mu_H) \propto T^{-3/2}$.

The surprisingly high Hall mobility —which we find unrealistic for polycrystalline, defect-rich films—and its sharp decrease upon increasing temperature, is best explained by large-polaron conduction. This conclusion is in agreement with one of the interaction mechanisms observed during muon spin relaxation,[19] and, in general, with the ionic character of the RE oxyhydrides,[12] which facilitates coupling between a charge and the crystal lattice.[30] Finally, we note that similar to this work, Hall-effect was reported to overestimate the polaron mobility by a factor of $10^2 - 10^3$ in Fe_2O_3-based epitaxial films and $BiVO_4$-based single crystals alike.[38]

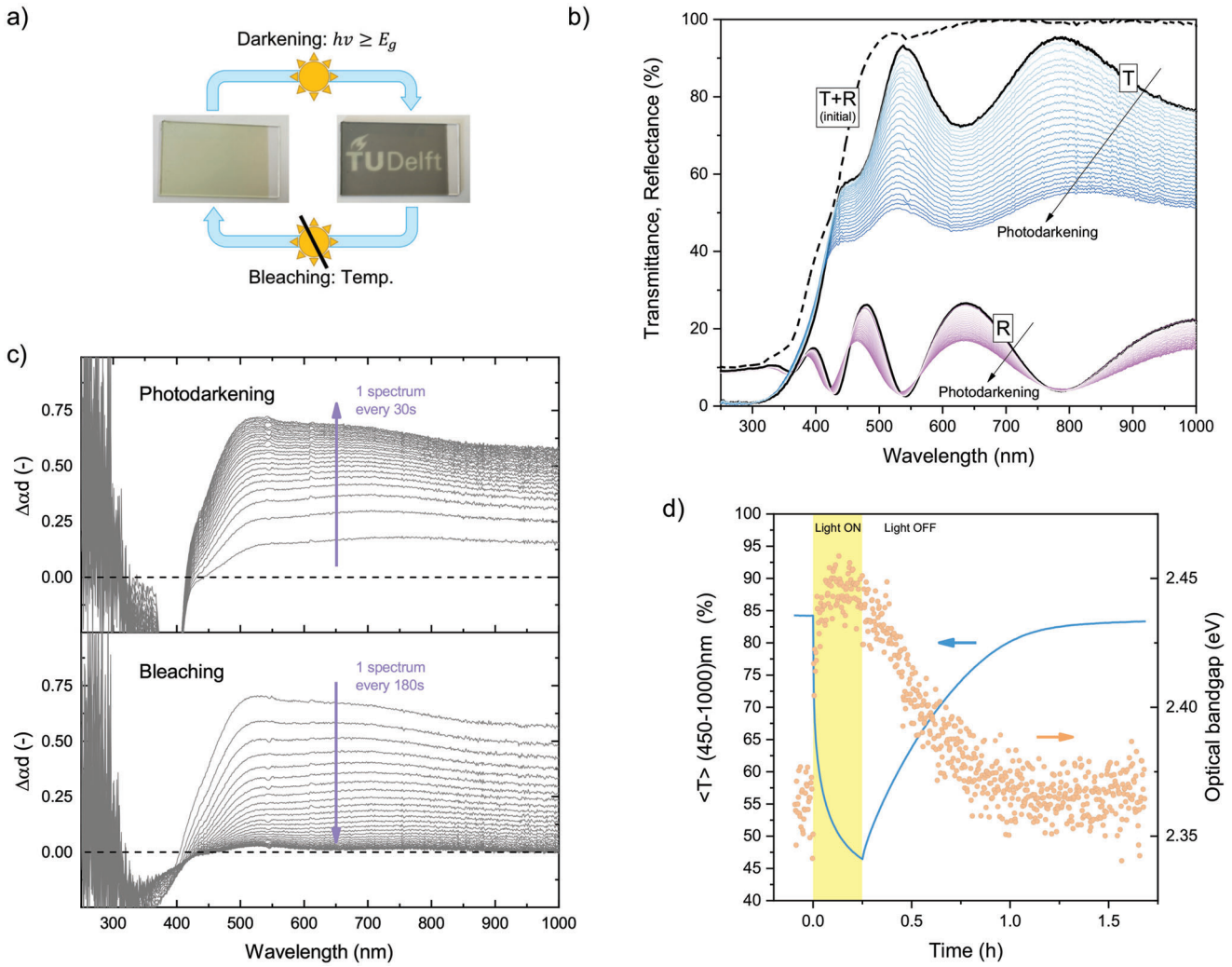

Figure 3. Overview of the photochromism in Gd oxyhydride thin films. a) Visual appearance and schematic representation of the competing photodarkening and temperature-activate bleaching processes. b) Examples of the transmittance (blue) and reflectance (purple) changes upon photodarkening. The initial properties, as well as their sum, complementary to the absorbance ($T + R = 1 - A$), are shown as black lines. c) Changes of optical absorption during photodarkening (top) and bleaching (bottom) with respect to the initial value ($\Delta\alpha = \alpha - \alpha_0$). d) Shift of the optical bandgap during the photochromic cycle.

3.2. Relation Between Photochromism and Photoconductivity

Mongstad et al.,[5] You et al.,[15] and Komatsu et al.,[22] have shown that photochromism in RE oxyhydride thin films is accompanied by a photo-induced change in conductivity. However, the connection between the two phenomena remained unexplored due to the challenge of acquiring time-dependent measurements under similar conditions. We do so here, relating the optical and electrical properties—synchronously measured at same temperature, atmosphere, and illumination conditions—on Gd oxyhydride thin films produced within the same deposition and with an identical history (i.e., same age and no previous light exposure).

A complete overview of the Gd oxyhydride photochromism is shown in **Figure 3**. When exposed to light of energy sufficient to initiate an interband transition ($hv > E_g$), the material undergoes a visually color-neutral darkening (Figure 3a), caused by a large decrease in transmittance accompanied by a small change of reflectance (Figure 3b). It is worth noting, that before illumination the material shows no optical absorption at energies below the bandgap, implying a negligible presence of optically active in-gap defects. Upon photodarkening, instead, the net increase in optical absorption spans a broad wavelength range, gently decreasing for longer wavelengths, and is rather featureless through the entire cycle of photodarkening and bleaching (Figure 3c). Lastly, the photochromic cycle is accompanied by a small widening of the optical bandgap (Figure 3d), something that might be due to the Burstein–Moss effect, that is, a full occupation of the states at the bottom of the conduction band.[39,40] Remarkably, this bandgap shift does not recover immediately after the light exposure ceases, but instead follows the slow kinetics of the photochromic effect, indicating that it is not solely due to a temporarily high concentration of electron-hole pairs excited under the photodarkening light.

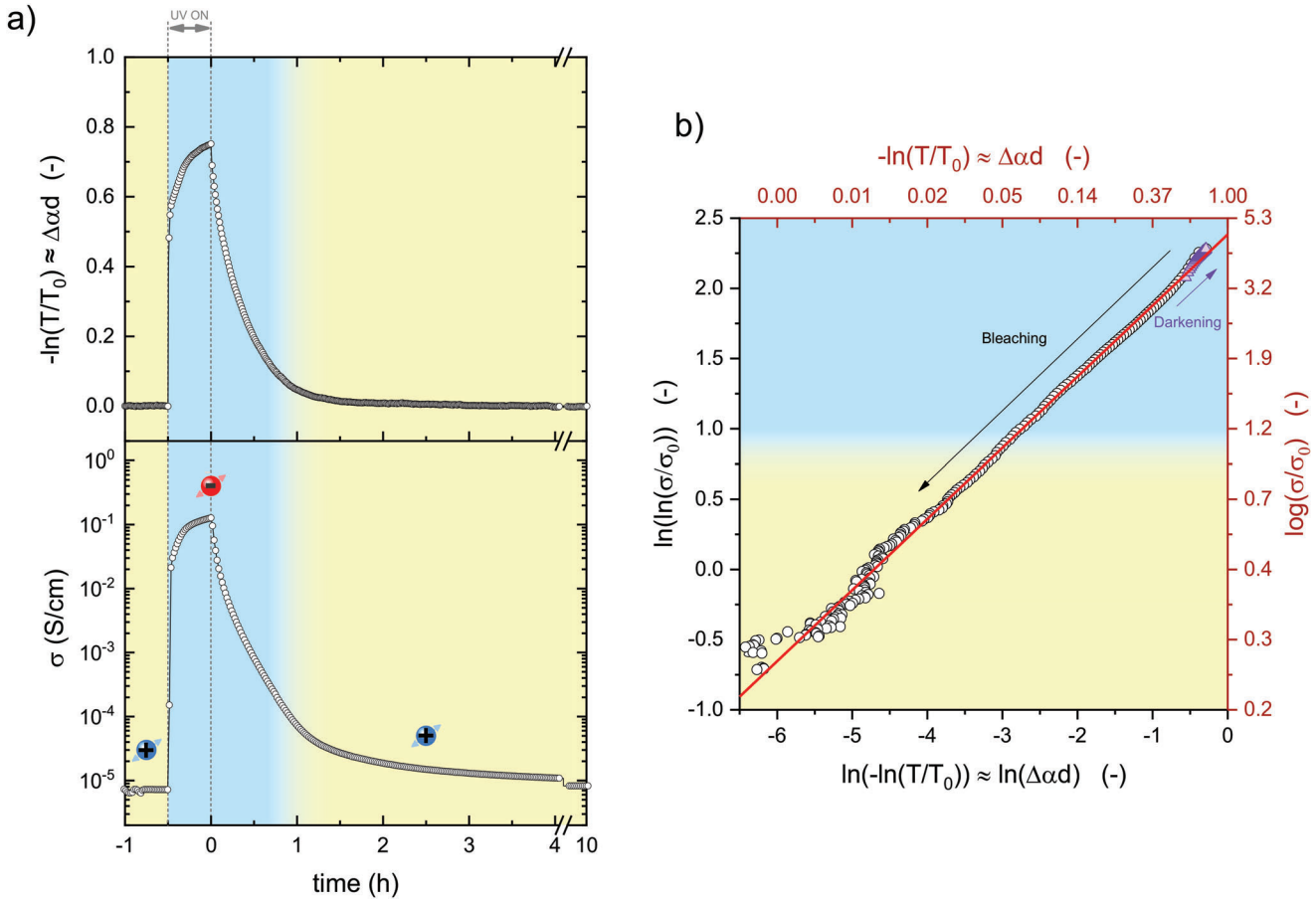

Figure 4. a) Photo-induced effects on relative optical transmittance (top) and material conductivity (bottom) of Gd oxyhydride measured at 303 K. Blue and red overlayed icons indicate the polarity of the dominant charge carriers at different stages of the cycle: holes when the material is in its transparent state, and electrons upon darkening. b) Relation (linearized) between the increase of optical absorption ($-\ln(T/T_0) \approx \Delta\alpha d$) and relative conductivity (σ/σ_0). The black points refer to the bleaching, while the purple ones to the darkening process. A linear fit based on Equation 1 is shown in red. In both panels, the background colors are guides to highlight the regime where optical absorption and conductivity are dominated by the photo-induced effects ($\sigma \gtrsim 10\ \sigma_0$; - blue), and the rest of the experimental range (yellow). Notably, the empirical Equation 1 well describes the relation between relative conductivity and optical absorption in both regimes.

How photochromism relates to changes in electronic conduction is shown in **Figure 4** a for data collected at 303K. The two phenomena follow a very comparable time dependence, pointing toward a common origin.

Looking at the conductivity of the material, after 30 min of illumination we find an increase from $\backsim 10^{-5}$ to $\backsim 10^{-1}$ S cm^{-1}. This change is 3 orders of magnitude larger than the one measured by Mongstad et al.[5] but roughly comparable to Komatsu et al.,[22] probably reflecting the different intensity of the photo-darkening light used by the different groups and the compositional differences of the samples. Additionally, differently from both studies, our results do not show signs of large irreversibility. Allowing enough bleaching time in the dark (e.g., 10 h at 303 K), we find that the conductivity of all samples largely returns to the initial value. We suspect that the irreversibility observed in the original study of Mongstad et al.[5] might be due to some degradation comparable to what we have observed for non-optimized contacts (see Supporting Information, Section II).

Unfortunately, accurate measures of the HE cannot be combined with illumination, as the permanent magnet would cover the light path. We could, however, measure the sample immediately after the 30 min of UV exposure, finding a polarity-switch in the Hall voltage that implies a change from p-type to n-type conductivity. The dominance of electron carriers in the photo-darkened state is in agreement with the Seebeck, β-NMR, and thermoelectric emission experiments of Komatsu et al.[22]

The relation between conductivity and relative optical transmittance is visualized in Figure 4b, where these two properties are plotted one against the other. The plot is linearized according to the best empirical relation that we could find, which is discussed in the following. To aid interpretation, we note that For a constant reflectance of the sample, an approximation largely verified (Figure 3b), it holds that $-\ln(T/T_0) \approx \Delta\alpha d$, where d is the thickness of the thin film, and $\Delta\alpha$ is the change in absorption coefficient due to the optically absorbing species formed by light exposure.[6] Thus, we find that the best empirical relation between σ and $\Delta\alpha d$ is:

$$\sigma(\Delta\alpha) = \sigma_0 \exp\left(B(\Delta\alpha d)^t\right) \quad (1)$$

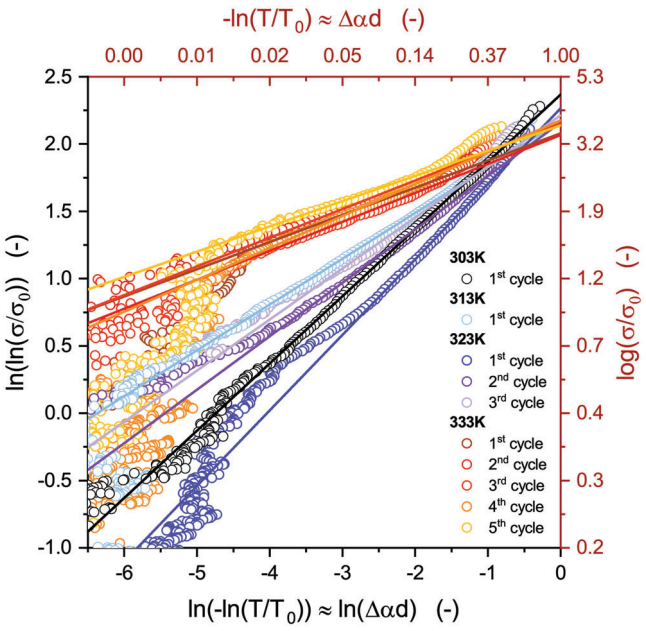

Figure 5. Relation (linearized) between the increase of optical absorption ($-\ln(T/T_0) \approx \Delta\alpha d$) and relative conductivity (σ/σ_0) during bleaching under different conditions. Linear fits based on Equation 1 are shown.

which in Figure 4b is linearized according to:

$$\ln\left(\ln\left(\frac{\sigma}{\sigma_0}\right)\right) = \ln(B) + t\ln(\Delta\alpha d) \quad (2)$$

Equation 1 is reminiscent of a stretched exponential function,[41] and states that the photo-conductivity is proportional to the conductivity of the oxyhydride in its initial transparent state (σ_0), while scaling exponentially with the increase of optical absorption. We suspect that the exponent t — as in the well-known stretched exponential function — might follow from the fact that the measured quantities σ and $\Delta\alpha d$ are average values with a certain variance. This variance might be due to how we defined these quantities (e.g., $\Delta\alpha$ is averaged over a broad wavelength range), but might also reflect a degree of local inhomogeneity within the sample. Finally, while the underlying physics behind the fitting parameter B remains unclear, we note that its value is largely unaffected by temperature and memory effect (**Figure 5** and **Table 1**). This indicates that photo-conductivity and photochromism have a single origin, and that their proportionality is not influenced by external factors nor by the kinetics of the process itself or the history of the sample.

While in the following discussion we cover our attempts of describing the experimental data in terms of other simpler functions and other established models (i.e., effective medium approximations, percolation phenomena, tunnelling, metal-insulator Anderson transition), here we note that only the empirical Equation 1 successfully captures the relation between σ and $\Delta\alpha d$.

The (i) dominance of negative charge carriers in the photo-darkened state, and (ii) the exponential relation between photoconductivity and optical absorption provide new insights into the mechanism of the RE oxyhydride photochromism. The process is initiated by the generation of an electron-hole pair via inter-band ($h\nu \geqslant E_g$) photo-excitation, but the subsequent formation of optically absorbing species and their identity remain topics of debate. At the time of writing, two hypotheses are under consideration. That is, the formation of local defects within the REO_xH_{3-2x} phase, and the phase segregation of a secondary absorbing/conductive phase. In the following we discuss these two hypotheses with the added insight from the transport measurements.

Table 1. Parameters B and t corresponding to the best fit of $\sigma = \sigma_0 \exp(B(\Delta\alpha d)^t)$ to the experimental data. Errors are estimated as $(max - min)/2$ by extending the fitting range to include the tails of the experimental data.

Temperature (K)	Cycle	B (-)	t (-)
303	1st	10.7 ± 0.3	0.50 ± 0.03
313	1st	8.7 ± 0.4	0.34 ± 0.06
323	1st	10 ± 1	0.56 ± 0.05
	2nd	8.7 ± 1.4	0.40 ± 0.09
	3rd	9 ± 1	0.38 ± 0.06
333	1st	8.0 ± 0.4	0.20 ± 0.04
	2nd	7.9 ± 0.4	0.22 ± 0.05
	3rd	8.6 ± 0.4	0.21 ± 0.03
	4th	8.8 ± 0.6	0.24 ± 0.03
	5th	8.5 ± 0.4	0.19 ± 0.03

3.2.1. Hypothesis of Long Living Small Defects

In this hypothesis, light exposure induces the formation of long-living small defects which trap either the electron or the hole and therefore affect the overall electrical properties of the thin film.

While trapping of the electron can result in the formation of color centres—as observed before in rare-earth compounds,[42,43] and indicated as the cause of photochromism in other inorganic materials[44,45]—the negative Hall voltage rules out this case and leaves trapping of the hole as the only possibility.

So far, three hole-trapping mechanisms have been suggested in RE oxyhydrides: the transformation of H^- ions into either neutral hydrogen, H^0,[46] or molecular hydrogen, H_2;[47] or the formation of hydroxide groups in the lattice.[22] The latter, in analogy with mayenite compounds.[48–51]

Whatever the nature of the hole trap, it is envisioned that the electrons excited to the conduction band—or equivalently in a newly formed electron band, following from an Anderson transition—are responsible for both optical absorption and conduction. This hypothesis is in line with the negative Hall potential, but fails to explain the relation between σ and $\Delta\alpha$, which would both be linearly proportional to the fraction of free electrons, and therefore to each other. Additionally, the photo-darkened state of the REO_xH_{3-2x} thin films shows modest reflectance and an absorption coefficient that decreases with the wavelength, aspects at odds with the typical metallic behavior and free carrier absorption in semiconductor materials ($\alpha(\lambda) \propto \lambda^p$, with $p > 0$).[52,53]

In the search for an exponential relation between increased optical absorption and conductivity, one might consider the

possibility of an Anderson metal-insulator transition, something known to occur in the related tri-hydrides $REH_{3-\delta}$ upon removal of a fraction ($\delta \gtrsim 0.3$) of the octahedral H.[25] Even this mechanism, however, does not provide a simple interpretation of the experimental $\sigma = \sigma_0 \exp(B(\Delta\alpha d)^t)$ relation. Indeed, the Anderson transition describes systems where disorder and/or defects localize the states near the Fermi energy, so that the electronic conduction—now diffusive rather than ballistic—decays as:

$$\sigma \propto \exp(-L/\xi) \tag{3}$$

where L is the distance that the electrons have to travel, and ξ a measure of the localization of their wave functions.[54,55] The shortcoming of the Anderson model in describing the experimental photoconductivity of the RE oxyhydrides is two-fold. First, the experimental photoconductivity is proportional to that of the material in the transparent (insulating) state (σ_0), while in the Anderson model is proportional to the conductivity of the metallic (conductive) state. Second, imagining that upon photodarkening new electronic states form ($L \propto 1/\Delta\alpha$) and/or that a further delocalization in space occurs ($\xi \propto \Delta\alpha$), results in a inverse negative exponential $\sigma \propto \exp(-1/\Delta\alpha)$ that cannot be reconciled with the experimental positive one.

3.2.2. Hypothesis of Metallic Phase Segregation

In this hypothesis, photo-darkening and photo-conductivity are explained by the segregation of a second phase with metallic properties. Proposed in analogy to the Cu-doped Ag-halide glasses—whose reversible photochromism is well known to depend on the segregation of plasmonic Ag particles[44,56–59]—this hypothesis is supported by the ellipsometry studies of Montero et al.,[17,18] who showed that the dielectric function of the darkened state could result from a small volume fraction ($v_{\%} = 1 - 10$ %) of metallic inclusions within the transparent matrix. Later, the formation/dissolution of metallic domains was further used as an argument to explain the reversible changes observed during positron annihilation spectroscopy with in situ illumination.[46]

Qualitatively, the merits of this hypothesis are several. From an optical perspective, the absorption would result from the plasmonic resonance localized at the surface of small metallic domains embedded in the dielectric RE oxyhydride matrix. An ensemble of metallic domains with different shapes and/or electronic properties (i.e., carrier concentration and/or effective mass) can, in fact, result in the broad spectral absorption of the darkened films.[6] From an electronic perspective, the formation of metallic domains within the thin film would explain the dominance of negative charge carriers and the increase of conductivity. In line with this idea, we note that during illumination, the Gd oxyhydride films reach a conductivity ($\backsim 10^{-1}$ Scm^{-1}) which is not far from that ($\backsim 10^{-2}$ Scm^{-1}) of a $GdO_xH_{3-2x}//GdH_x$ mixed-phase sample purposely produced as a reference (Figure S8, Supporting Information). Furthermore, the light-induced volume contraction, and the slow[6,13] temperature activated[20,21] kinetics would follow from the necessary structural rearrangements. The time dependence of the bleaching can be connected to the average rate of disappearance of the metallic domains.

Despite the fact that this hypothesis provides a compelling explanation of the optical changes, a small fraction of embedded and isolated metallic domains has only a marginal impact on the overall electronic conductivity.[60,61] Indeed, if the photoconductivity were the result of segregated metallic domains alone, these could account for the experimental $\backsim 10^4$-fold increase only by forming a percolated (i.e., connected) network throughout the otherwise poorly conductive matrix—something that for an homogeneous dispersion of spherical metallic domains occurs only at a much higher fraction of the total material, on the order of $\backsim$30% according to the Bruggerman effective medium approximation (see Supporting Information, Section IV). Such amount of metallic phase would almost completely suppress the optical transmittance of the film, and is thus incompatible with the observed properties (e.g., Figure 3d). It should be noted, however, that estimating the critical volume fraction at which percolation occurs is a highly complicated problem,[62,63] and while effective medium approximations like Bruggerman provide a qualitative image, experimental thresholds are system-dependent and they typically fall in the rather broad range of 15–50%.[64–69] Additionally, for our porous and polycrystalline films it is possible that the nucleation of a second phase preferentially occurs along energetically favorable regions, such as grain boundaries or volume defects. Therefore we relax the assumptions of homogeneous dispersion and spherical domains, and consider the hypothesis that percolation might occur at any arbitrarily low levels of phase segregation. However, even in this scenario, we are still unable to describe the experimental data in the framework of percolation phenomena. Percolation theory predicts the conductivity of the composite as:[63,70,71]

$$\sigma = \sigma_0 \left(\frac{p_c}{p_c - \phi} \right)^s \tag{4}$$

where σ_0 is the conductivity of the insulating matrix, ϕ the volume fraction of metallic inclusions, p_c the percolation threshold, and s an exponent which depends on the topology of the connected network. Equation 4 diverges un-physically as the volume fraction of the metallic phase approaches the amount sufficient for percolation ($\phi \rightarrow p_c$), but describes correctly the initial phase of the *insulator-to-conductor* transition — a regime to which our experimental case should belong given the maximum photoconductivity observed, which is orders of magnitude smaller than that of a typical metal. The power law above cannot be expanded and approximated to an exponential function, and taking the increased optical absorption as proportional to the volume fraction of metallic domains $\phi \propto \Delta\alpha$, it does not fit the experimental data even for unconstrained values of p_c and s (Figure S11, Supporting Information).

Finally, going beyond classical descriptions, we consider the case of tunnelling conductivity between the metallic domains,[69,72–74] which at high temperatures exponentially decays with the height of the tunnelling barrier (X) and the separation (s) between them:

$$\sigma \propto \exp(-2Xs) \tag{5}$$

While the exponential functionality is attractive, this model encounters the same two limits of the Anderson model. First, the model is proportional to the most conductive phase, while it is experimentally found that the photoconductivity is proportional to

that of the material in its transparent (insulating) state. Second, imagining that more and more metallic particles nucleate upon photodarkening—thus lowering the average separation ($s \propto 1/\Delta\alpha$) — results in a functionality of the form $\sigma \propto \exp(-1/\Delta\alpha)$, which is incompatible with the experimental one.

4. Conclusion

In this work, we have surveyed the transport properties of photochromic Gd oxyhydride thin films produced via air oxidation of reactively sputtered Gd dihydrides.

The electical conductivity of these films is rather low ($\sigma_0 \approx 10^{-5}$ Scm^{-1} at room temperature), and the mechanism of charge transport is identified as p-type large-polaron conduction by HE measurements. Upon illumination, however, the material undergoes optical photodarkening and its conductivity increases by several orders of magnitude (up to $\sigma \approx 10^{-1}$ Scm^{-1}), this time dominated by negative charge carriers.

We find that photochromism and photoconductivity clearly have a single origin and are connected by an exponential relation, $\sigma = \sigma_0 \exp(B(\Delta\alpha d)^t)$. Such relation cannot be explained in the framework of any of the two mechanisms proposed to describe the photochromic effect, that is (i) generation of small defects, and (ii) segregation of metallic domains. This indicates that no single species formed upon illumination can simultaneously explain optical and electrical changes, and forces us to contemplate more complex explanations where the excited electron and the hole both induce an electronic change. Light exposure might involve the segregation of sparse metallic domains together with connected changes within the RE oxyhydride matrix, such as defects generation and/or a shift of the Fermi level. In this case, the sparse metallic domains would be largely responsible for the optical absorption but only marginally for the increased conductivity, while the net increase of negative charge carriers would occur in the transparent RE oxyhydride matrix. A reversible change of the matrix is further indicated by the shift of optical bandgap, that within the proposed picture is explained via the Burstein-Moss effect.

Supporting Information

Supporting Information is available from the Wiley Online Library or from the author.

Acknowledgements

The authors thank Dr. Stephan Eijt, Dr. Steffen Cornelius, Marcel Bus, and Melanie Beek for insightful discussions, and Dr. Vasyl P. Kunets for the technical support with the MMR system. This work was partially supported by the Open Technology research program with project number 13282 and by the Mat4Sus research program with project number 680.M4SF.034; both financed by the Dutch Research Council (NWO).

Conflict of Interest

The authors declare no conflict of interest.

Data Availability Statement

The data that support the findings of this study are available from the corresponding author upon reasonable request.

Keywords

gadolinium, hydrides, oxyhydrides, photochromism, photoconductivity, polarons

Received: November 8, 2022
Revised: April 28, 2023
Published online:

[1] H. Kageyama, K. Hayashi, K. Maeda, J. P. Attfield, Z. Hiroi, J. M. Rondinelli, K. R. Poeppelmeier, *Nat. Commun.* **2018**, *9*, 772.
[2] N. F. Borrelli, in *Photosensitive Glass and Glass-Ceramics*, CRC Press, Boca Raton, FL, USA **2017**.
[3] A. Dotsenko, L. Glebov, V. A. Tsechomsky, in *Physics and Chemistry of Photochromic Glasses*, CRC Press, Boca Raton, FL, USA **1998**.
[4] A.-L. Leistner, Z. L. Pianowski, *Eur. J. Org. Chem.* **2022**, *2022*, e202101271.
[5] T. Mongstad, C. Platzer-Björkman, J. P. Maehlen, L. P. Mooij, Y. Pivak, B. Dam, E. S. Marstein, B. C. Hauback, S. Z. Karazhanov, *Sol. Energy Mater. Sol. Cells* **2011**, *95*, 3596.
[6] F. Nafezarefi, H. Schreuders, B. Dam, S. Cornelius, *Appl. Phys. Lett.* **2017**, *111*, 103903.
[7] S. Cornelius, G. Colombi, F. Nafezarefi, H. Schreuders, R. Heller, F. Munnik, B. Dam, *J. Phys. Chem. Lett.* **2019**, *10*, 1342.
[8] S. Adalsteinsson, M. Moro, D. Moldarev, S. Droulias, M. Wolff, D. Primetzhofer, *Nucl. Instrum. Methods Phys. Res., Sect. B* **2020**, *485*, 36.
[9] D. Chaykina, F. Nafezarefi, G. Colombi, S. Cornelius, L. J. Bannenberg, H. Schreuders, B. Dam, *J. Phys. Chem. C* **2022**, *126*, 2276.
[10] D. Chaykina, G. Colombi, H. Schreuders, B. Dam, *AIP Advances* **2023**, *13*, 055211.
[11] G. Colombi, S. Cornelius, A. Longo, B. Dam, *J. Phys. Chem. C* **2020**, *124*, 13541.
[12] G. Colombi, R. Stigter, D. Chaykina, S. Banerjee, A. P. M. Kentgens, S. W. H. Eijt, B. Dam, G. A. de Wijs, *Phys. Rev. B* **2022**, *105*, 054208.
[13] G. Colombi, T. De Krom, D. Chaykina, S. Cornelius, S. W. H. Eijt, B. Dam, *ACS Photonics* **2021**, *8*, 709.
[14] C. C. You, T. Mongstad, J. P. Maehlen, S. Karazhanov, *Appl. Phys. Lett.* **2014**, *105*, 031910.
[15] C. C. You, T. Mongstad, E. S. Marstein, S. Z. Karazhanov, *Materialia* **2019**, *6*, 100307.
[16] K. Fukui, S. Iimura, T. Tada, S. Fujitsu, M. Sasase, H. Tamatsukuri, T. Honda, K. Ikeda, T. Otomo, H. Hosono, *Nat. Commun.* **2019**, *10*, 2578.
[17] J. Montero, F. A. Martinsen, M. García-Tecedor, S. Z. Karazhanov, D. Maestre, B. Hauback, E. S. Marstein, *Phys. Rev. B* **2017**, *95*, 201301.
[18] J. Montero, S. Z. Karazhanov, *Phys. Status Solidi A* **2018**, *215*, 1701039.
[19] D. Chaykina, T. de Krom, G. Colombi, H. Schreuders, A. Suter, T. Prokscha, B. Dam, S. Eijt, *Phys. Rev. B* **2021**, *103*, 224106.
[20] E. M. Baba, P. M. Weiser, E. z. Zayim, S. Karazhanov, *Phys. Status Solidi RRL* **2021**, *15*, 2000459.
[21] D. Chaykina, I. Usman, G. Colombi, H. Schreuders, B. Tyburska-Pueschel, Z. Wu, S. W. H. Eijt, L. J. Bannenberg, G. A. de Wijs, B. Dam, *J. Phys. Chem. C* **2022**, *126*, 14742.
[22] Y. Komatsu, R. Shimizu, R. Sato, M. Wilde, K. Nishio, T. Katase, D. Matsumura, H. Saitoh, M. Miyauchi, J. R. Adelman, R. M. L. McFadden, D. Fujimoto, J. O. Ticknor, M. Stachura, I. McKenzie, G. D. Morris, W. A. MacFarlane, J. Sugiyama, K. Fukutani, S. Tsuneyuki, T. Hitosugi, *Chem. Mater.* **2022**, *34*, 3616.
[23] E. S. Kooij, A. T. M. van Gogh, R. Griessen, *J. Electrochem. Soc.* **1999**, *146*, 2990.

[24] A. F. T. Hoekstra, A. S. Roy, T. F. Rosenbaum, R. Griessen, R. J. Wijngaarden, N. J. Koeman, *Phys. Rev. Lett.* **2001**, *86*, 5349.
[25] K. K. Ng, F. C. Zhang, V. I. Anisimov, T. M. Rice, *Phys. Rev. B* **1999**, *59*, 5398.
[26] A. T. M. van Gogh, D. G. Nagengast, E. S. Kooij, N. J. Koeman, J. H. Rector, R. Griessen, C. F. J. Flipse, R. J. J. G. A. M. Smeets, *Phys. Rev. B* **2001**, *63*, 195105.
[27] M. Zubkins, I. Aulika, E. Strods, V. Vibornijs, L. Bikse, A. Sarakovskis, G. Chikvaidze, J. Gabrusenoks, H. Arslan, J. Purans, *Vacuum* **2022**, 111218.
[28] L. J. Van der Pauw, *Phylips Res. Rep.* **1958**, *13*, 1.
[29] M. Cesaria, A. P. Caricato, M. Martino, *J. Opt.* **2012**, *14*, 105701.
[30] C. Franchini, M. Reticcioli, M. Setvin, U. Diebold, *Nat. Rev. Mater.* **2021**, *6*, 560.
[31] D. Emin, in *Polarons*, Cambridge University Press, Cambridge **2012**.
[32] E. H. Hall, *Am. J. Math.* **1879**, *2*, 287.
[33] C. Kittel, in *Introduction to Solid State Physics*, 9th Ed., John Wiley and Sons, Hoboken, NJ, USA **2018**.
[34] K. Bolotin, K. Sikes, Z. Jiang, M. Klima, G. Fudenberg, J. Hone, P. Kim, H. Stormer, *Solid State Commun.* **2008**, *146*, 351.
[35] Y. Yongbo, G. Gaurav, A. A. L., A. P. Zoombelt, S. C. B. Mannsfeld, C. Jihua, N. Dennis, T. M. F., Huang, Jinsong, B. Zhenan, *Nat. Commun.* **2014**, *5*, 351.
[36] P. Heremans, A. K. Tripathi, A. de Jamblinne de Meux, E. C. P. Smits, B. Hou, G. Pourtois, G. H. Gelinck, *Adv. Mater.* **2016**, *28*, 4266.
[37] D. Joshi, R. Srivastava, *Solar Cells* **1984**, *12*, 337.
[38] A. J. E. Rettie, W. D. Chemelewski, D. Emin, C. B. Mullins, *J. Phys. Chem. Lett.* **2016**, *7*, 471.
[39] E. Burstein, *Phys. Rev.* **1954**, *93*, 632.
[40] T. S. Moss, *Proc. Phys. Soc., Sect. B* **1954**, *67*, 775.
[41] D. C. Johnston, *Phys. Rev. B* **2006**, *74*, 184430.
[42] D. L. Staebler, S. E. Schnatterly, *Phys. Rev. B* **1971**, *3*, 516.
[43] H. Bill, G. Calas, *Phys. Chem. Miner.* **1978**, *3*, 117.
[44] R. Araujo, *Mol. Cryst. Liq. Cryst. Sci. Technol., Sect. A* **1997**, *297*, 1.
[45] T. He, J. Yao, *J. Photochem. Photobiol., C* **2003**, *4*, 125.
[46] Z. Wu, T. de Krom, G. Colombi, D. Chaykina, G. van Hattem, H. Schut, M. Dickmann, W. Egger, C. Hugenschmidt, E. Brück, B. Dam, S. W. H. Eijt, *Phys. Rev. Mater.* **2022**, *6*, 065201.
[47] J. Chai, Z. Shao, H. Wang, C. Ming, W. Oh, T. Ye, Y. Zhang, X. Cao, P. Jin, S. Zhang, Y.-Y. Sun, *Sci. China Mater.* **2020**, *63*, 1579.
[48] K. Hayashi, S. Matsuishi, T. Kamiya, M. Hirano, H. Hosono, *Nature* **2002**, *419*, 1476.
[49] K. Hayashi, *J. Phys. Chem. C* **2011**, *115*, 11003.
[50] K. Hayashi, P. V. Sushko, Y. Hashimoto, A. L. Shluger, H. Hosono, *Nat. Commun.* **2014**, *5*, 2041.
[51] K. Hayashi, H. Hosono, *Phys. Chem. Chem. Phys.* **2016**, *18*, 8186.
[52] K. Seeger, in *Semiconductor Physics: An introduction*, 9th Ed., Springer, New York, NY, USA **2004**.
[53] R. M. Culpepper, J. R. Dixon, *J. Opt. Soc. Am.* **1968**, *58*, 2578.
[54] P. A. Lee, T. V. Ramakrishnan, *Rev. Mod. Phys.* **1985**, *57*, 287.
[55] E. Abrahams, in *50 Years of Anderson Localization*, World Scientific, Singapore **2010**.
[56] R. J. Araujo, *Contemp. Phys.* **1980**, *21*, 77.
[57] N. F. Borrelli, J. B. Chodak, G. B. Hares, *J. Appl. Phys.* **1979**, *50*, 5978.
[58] T. Seward, *J. Non-Cryst. Solids* **1980**, *40*, 499.
[59] C. L. Marquardt, J. F. Giuliani, R. T. Williams, *J. Appl. Phys.* **1976**, *47*, 4915.
[60] D. A. G. Bruggeman, *Ann. Phys.* **1935**, *416*, 636.
[61] O. Stenzel, in *The Physics of Thin Film Optical Spectra*, Springer, New York, NY, USA **2005**.
[62] M. Hori, F. Yonezawa, *J. Phys. C: Solid State Phys.* **1977**, *10*, 229.
[63] D. Stauffer, A. Aharony, in *Introduction To Percolation Theory: Second Edition*, (2nd ed.), Taylor & Francis, Abingdon, UK **1992**.
[64] R. Viswanathan, M. B. Heaney, *Phys. Rev. Lett.* **1995**, *75*, 4433.
[65] M. B. Heaney, *Phys. A* **1997**, *241*, 296.
[66] J. Wu, D. S. McLachlan, *Phys. Rev. B* **1997**, *56*, 1236.
[67] M. Ambrozic, A. Lazar, A. Kocjan, *J. Eur. Ceram. Soc.* **2020**, *40*, 1684.
[68] J. Martinelli, F. Sene, *Ceram. Int.* **2000**, *26*, 325.
[69] D. Toker, D. Azulay, N. Shimoni, I. Balberg, O. Millo, *Phys. Rev. B* **2003**, *68*, 041403.
[70] B. I. Shklovskii, A. L. Efros, in *Electronic Properties of Doped Semiconductors*, Springer Berlin, Heidelberg **1984**.
[71] W.-Z. Cai, S.-T. Tu, J.-M. Gong, *J. Compos. Mater.* **2006**, *40*, 2131.
[72] J. E. Morris, A. Mello, C. J. Adkins, *MRS Online Proc. Libr.* **1990**, *195*, 181.
[73] J. V. Mantese, W. A. Curtin, W. W. Webb, *Phys. Rev. B* **1986**, *33*, 7897.
[74] B. Abeles, P. Sheng, M. Coutts, Y. Arie, *Adv. Phys.* **1975**, *24*, 407.